The Separation and Identification of Polyoxometalate Mixtures

Stephanie Peterson

Advisor: Dr. Keith Marek

Abstract: Various techniques can be used to study polyoxometalates (POMs) in pure form, but it can sometimes be difficult to crystallize POMs from a mixture. Often, mixtures of various sized anions are formed in synthesis, and identification of the mixtures is essential to the understanding of the chemistry of these systems. In this project, ion chromatography (IC) and nuclear magnetic resonance (NMR) spectroscopy are focused on to analyze known and unknown POM mixtures. The intentions were to use ion chromatography to identify the charge and the number of components present within a solution because IC is a useful method that separates components in a solution. When the project was first started, four goals were identified to (1) make known compounds and analyze them through IC to determine their characteristic absorption properties, (2) develop a technique that can be applied to POMs by analyzing known single and multiple component mixtures, (3) adapt this procedure to the unknown solutions to determine the components (by using data from the known compounds, a practical concentration range can be found by identifying the retention factor at different concentrations), and (4) correlate the results with results from NMR analysis for more specific information. As the research was done, the overall project took different directions due to the circumstances encountered. The following will explain the research in detail along with the conclusions.

Introduction: POMs are metal oxygen containing anions formed by adding a base to metal oxides or an acid to high pH oxoanions. The ability of the early transition metals (such as V, Nb, Ta, Mo,a and W) in their highest oxidation states to form metal-oxygen cluster anions is one definition given to explain POMs (7). POMs include a large class of nanosize metal-oxygen

cluster anions either of the form $[M_mO_y]^{p-}$, isopolyanions, or of the form $[X_xM_mO_y]^{q-}$ ($x \leq m$), which are heteropoly anions (11). POMs with three or more non-oxo atoms are found in two regions of the periodic table, the early transition metals and certain p-block elements, as seen in Figure 1 (16).

H																	*He*
Li	*Be*											**B**	*C*	*N*	*O*	*F*	*Ne*
Na	*Mg*											*Al*	**Si**	**P**	*S*	*Cl*	*Ar*
K	*Ca*	*Sc*	*Ti*	**V**	**Cr**	*Mn*	*Fe*	*Co*	*Ni*	*Cu*	*Zn*	*Ga*	**Ge**	**As**	*Se*	*Br*	*Kr*
Rb	*Sr*	*Y*	*Zr*	**Nb**	**Mo**	*Tc*	*Ru*	*Rh*	*Pd*	*Ag*	*Cd*	*In*	*Sn*	**Sb**	**Te**	**I**	*Xe*
Cs	*Ba*	*La*	*Hf*	**Ta**	**W**	*Re*	*Os*	*Ir*	*Pt*	*Au*	*Hg*	*Tl*	*Pb*	*Bi*	*Po*	*At*	*Rn*
Fr	*Ra*	*Ac*															

Figure 1. Periodic Table of the Elements showing the metals and elements that usually occur in POMs.

POMs are by far, mostly formed by Mo, W, and V, usually in their highest oxidation states (13). The creation of POMs takes place during synthesis when mixtures of various-sized anions are formed by a process called self-assembly (15). POMs take on many structures, but all of the anions in this study have the so-called Keggin structure, $H_3PW_{12}O_{40}\cdot 5H_2O$, shown in Figures 2 and 3 (15).

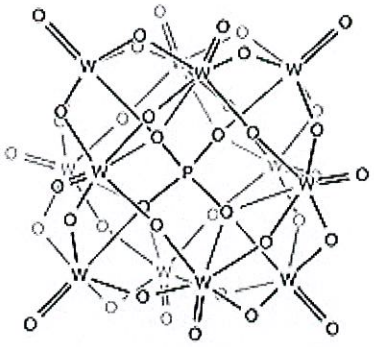

Figure 2. Keggin structure

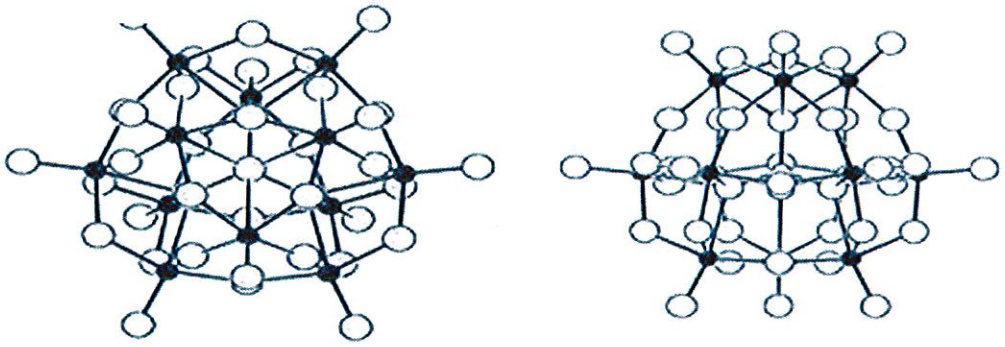

(a) (b)

Figure 3. Other representations of the Keggin structure, (a) looking from C_3 axis (b) viewing perpendicular to C_3.

"In 1933, Keggin's determination of the structure of the tungstophosphate anion in $H_3[PW_{12}O_{40}]\cdot 6H_2O$ opened the era of structurally characterized POMs" (13). This structure confirmed the general principles previously suggested by Pauling (13). There is a variety of POM structures that exist and is easiest to understand the Keggin structure to be the 'parent' structure and the many other POM structures to be 'derivatives' (11). "POM structures are governed by two general principles, the most important one being the first:

- Each metal atom occupies an MO_n coordination polyhedrom (most commonly an octahedron or square pyramid) in which the metal atoms are displaced, as a result of MO π-bonding, towards those polyhedral vertices that form the surface
- The structures are generated by linking MO_n polyhedra in different ways, producing different types of faces on the surfaces" (15).

Before the chemistry of POMs existed, anions were of interest. In 1826, Berzelius was credited of what is now known to be the dodecamolydophosphate anion, $[PMo_{12}O_{40}]^{3-}$ (said by Pope, Müller, Borrás-Almenar, and Coronado in reference 16) or first heteropoly salt, ammonium 12-molybdophosphate (11). At the time, molybdenum was a newly-recognized element and Berzelius explained how he observed the formation of yellow and reduced blue compounds by the addition of phosphate and arsenate mixed in molybdic acid (according to

Pope, Müller, Borrás-Almenar, and Coronado in reference 16). It wasn't until the time span of 1862-1864 when Marignac made the first systematic study of POMs(16). He prepared and correctly analyzed two isomers of 12-tungstosilic acid, what was called "tungstosilicic acid" and "silicotungstic acid" but is now known as α and β isomers, and several salts (16). It was in the early 1900s when heteropoly compounds were prepared and analyzed. By 1908, about 750 heteropoly compounds were reported. This began the surge of research on POMs throughout the 1900s.

Due to the unusually large size of the POM structures, POMs run the risk of being decomposed to monomeric species in basic solution (5). If a POM is 'defected,' the newly formed structures are termed lacunary, particularly meaning 'hole in compound'. "Typically, metal cations are bound into the cavity generated by the loss of MO^{4+} from the Keggin structure" (13). Especially with analysis of ion chromatography (IC), where hydroxide (^{-}OH) is used as the eluent in the system to remove the anion species, the basic hydroxide runs the possibility of destroying the POM and creating a lacunary species, in which nothing would be detectable.

Polyoxometalates are formed in pH regions intermediate between low pH acidic oxide and high pH metal oxoanions, shown in the following reaction:

$$XO_4^{n-} + H^+ \rightarrow (XO_3)OH$$

$$2(XO_3)OH \rightarrow {}^{-}O_3X\text{-}O\text{-}XO^{-}_3 + H_2O$$

Experimental Section: For the synthesis of POMs, various experiments were carried out following the literature provided from advisor (6). See 'Appendix' for further details on preparation of analyzed compounds.

Infrared spectroscopy used as an indicator of the purity and identity of the products. After the preparation of the six compounds, infrared spectroscopy (abbreviated IR) was used as confirmation of production of the products with the literature data.

Figure 5. The three colorful phosphorus-containing solids, $K_4[\alpha\text{-}PV^VW_{11}O_{40}]$, $Cs_6[\alpha\text{-}1,2,3\text{-}PV_3W_9O_{40}]$, and $Cs5[\gamma\text{-}PV_2W_{10}O_{40}]$, used for research.

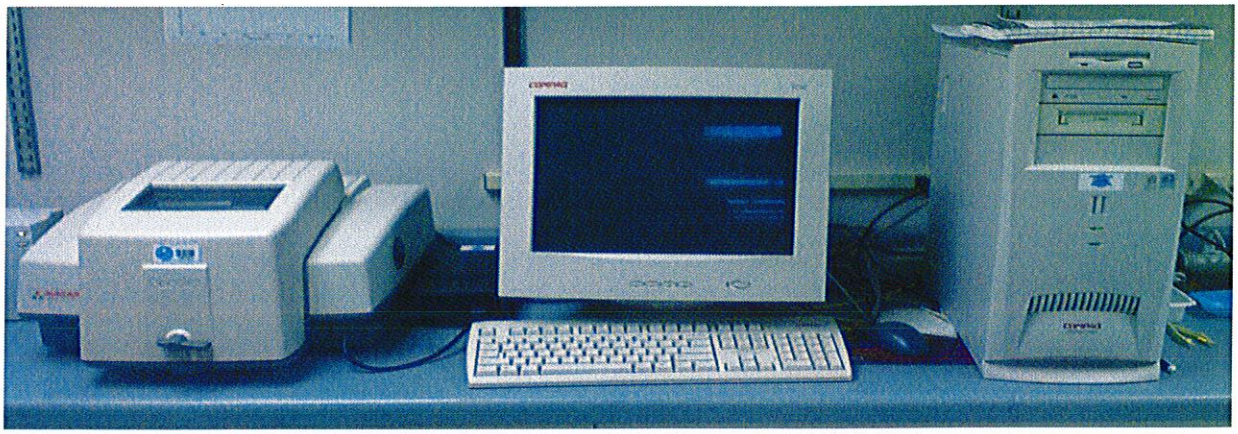

Figure 4. Infrared spectrometer at BSU.

IR deals with the infrared portion of the electromagnetic magnetic spectrum that provides a simple and prompt instrumental technique that gives evidence for the presence of various functional groups (18). Infrared radiation, which can not be seen but can be sensed in the form of heat, is what causes atoms within compounds to vibrate with increased amplitude about covalent bonds that connect the two (18). With the vibrations being increased, the IR absorption

by the organic molecules will occur at specific frequencies depending on the characteristics of the type of bonds present in the certain functional groups of the molecule being analyzed (18). The observed data from taking the IR spectra included the following:

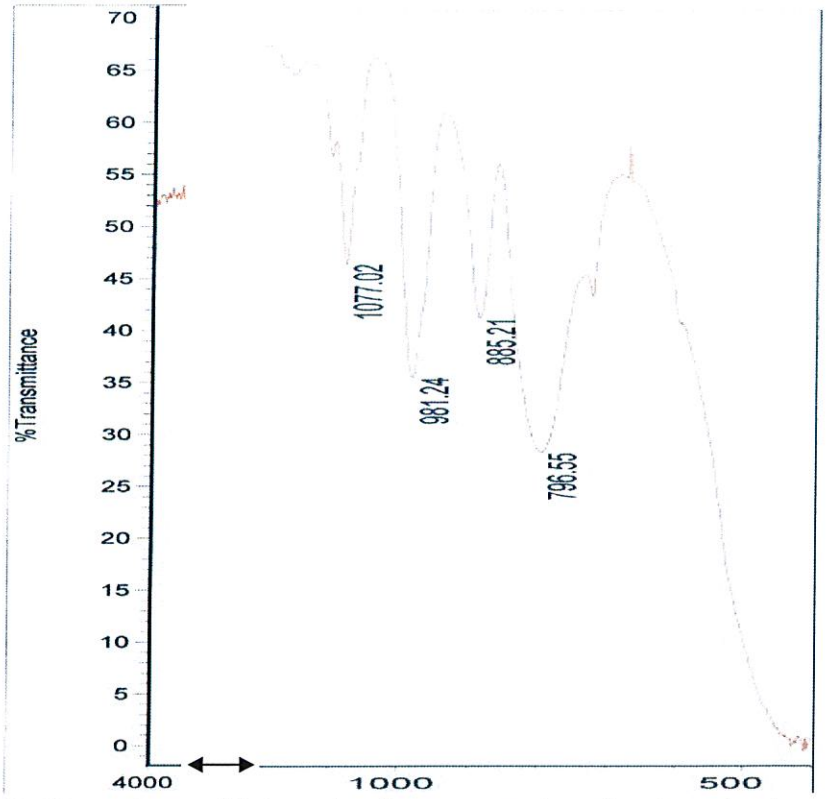

Figure 6. IR spectrum of tetrapotassium α-vanadoundecatungstophosphate $K_4[\alpha\text{-}PV^VW_{11}O_{40}]$.

$K_4[\alpha\text{-}PV^VW_{11}O_{40}]$ IR Spectrum	
Literature values (cm^{-1}):	Experimental values (cm^{-1}):
1101 (m)	present
1077 (s)	1077.02
1065 (sh)	present
982 (s)	981.24
881 (s)	885.21

Table 1. Comparison between the literature and experimental values.

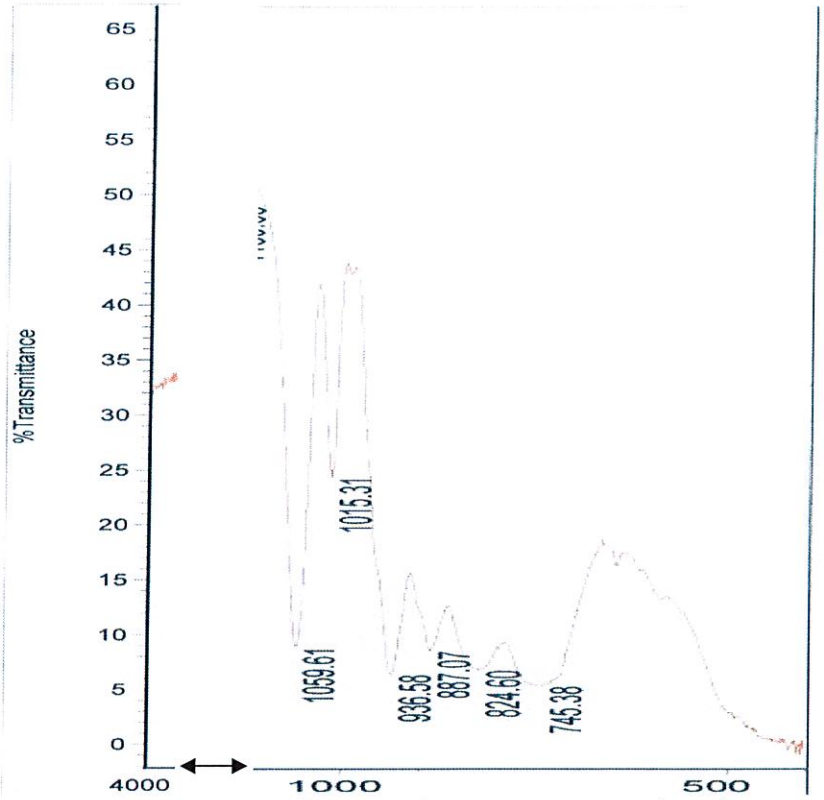

Figure 7. IR spectrum of nonasodium nonatungstophosphate $Na_9[PW_9O_{34}]$.

$Na_9[PW_9O_{34}]$ IR Spectrum	
Literature values (cm^{-1}):	Experimental values (cm^{-1}):
1052 (s)	1059.61
1017 (m)	1015.31
941 (s)	936.58
886 (m)	887.07
836 (s)	824.60
740-760 (s, broad)	745.38

Table 2. Comparison between the literature and experimental values. All of the literature values were detected and very similar.

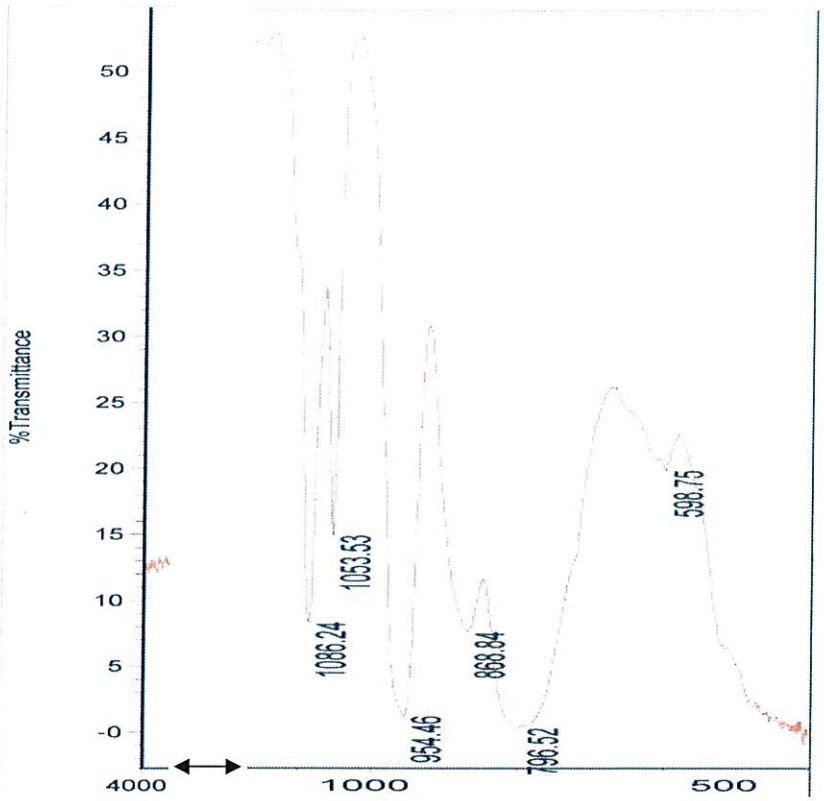

Figure 8. IR spectrum of hexacesium α-1,2,3-trivanadononatungstophosphate $Cs_6[\alpha\text{-}1,2,3\text{-}PV_3W_9O_{40}]$.

$Cs_6[\alpha\text{-}1,2,3\text{-}PV_3W_9O_{40}]$ IR Spectrum	
Literature values (cm^{-1}):	Experimental values (cm^{-1}):
1085 (s)	1086.24
1053 (m)	1053.53
953 (vs, sh)	954.46
789 (vs, br)	796.52

Table 3. Comparison between the literature and experimental values. All of the literature values were detected in the experimental values.

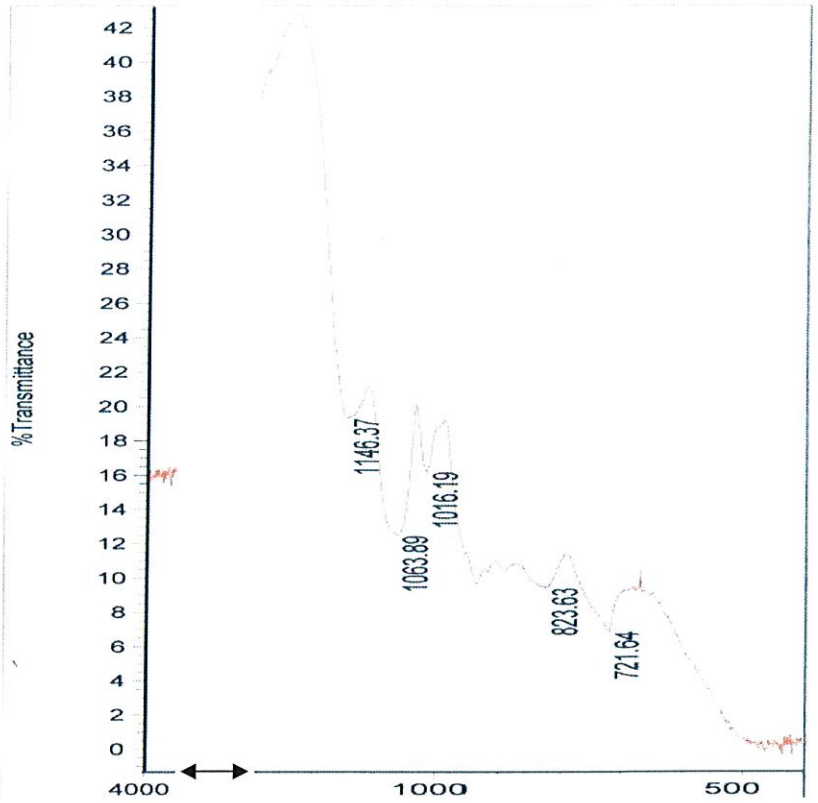

Figure 9. IR spectrum of hexacesium pentatungstodiphosphate $Cs_6[P_2W_5O_{23}]$.

$Cs_6[P_2W_5O_{23}]$ IR Spectrum	
Literature values (cm^{-1}):	Experimental values (cm^{-1}):
1180 (m)	
1153 (m)	1146.37
1048 (s)	1063.89
986 (w)	1016.19
893 (vs, shoulders)	
801 (w)	823.63
686 (s)	721.64

Table 4. Comparison between the literature and experimental values. Not all literature values were detected and not very close to what is expected.

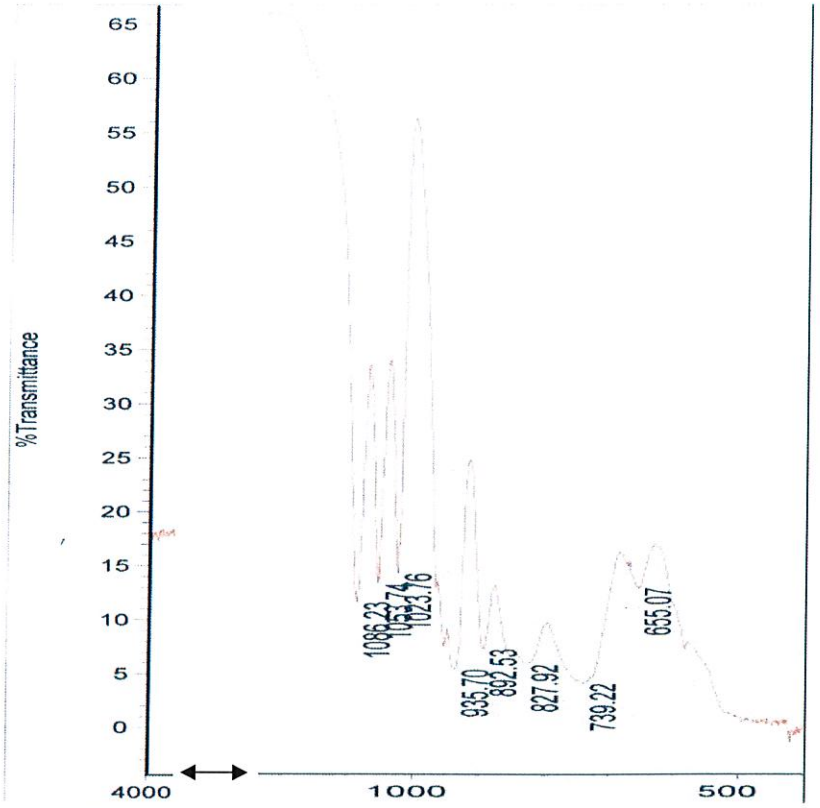

Figure 10. IR spectrum of heptacesium decatungstophosphate $Cs_7[PW_{10}O_{36}]$.

$Cs_7[PW_{10}O_{36}]$ IR Spectrum	
Literature values (cm^{-1}):	Experimental values (cm^{-1}):
1086 (ms)	1086.23
1053 (m)	1053.74
1023 (m)	1023.76
965 and 952 (sh)	present
937 (s)	935.70
892 (s)	892.53
850 (m)	present
830 (m)	827.92
735 (vs, br)	739.22

Table 5. Comparison between the literature and experimental values.

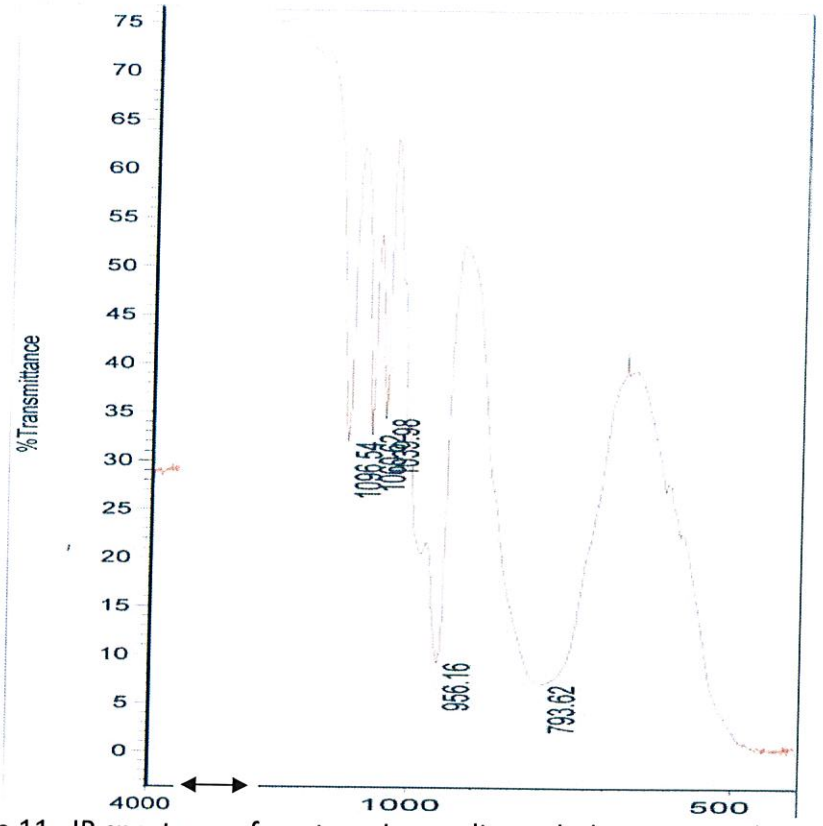

Figure 11. IR spectrum of pentacesium γ-divanadodecatungstophosphate $Cs_5[\gamma\text{-}PV_2W_{10}O_{40}]$.

$Cs_5[\gamma\text{-}PV_2W_{10}O_{40}]$ IR Spectrum	
Literature values (cm^{-1}):	Experimental values (cm^{-1}):
1096 (m)	1096.54
1060 (m)	1060.62
1040 (m)	1039.98
1007 (sh)	present
985 (sh)	present
954 (s)	956.16
766 (vs, br)	

Table 6. Comparison between the literature and experimental values. All except one of the experimental values correspond to the literature values.

The accurate IR spectra of the six samples supported efforts to proceed further with the research.

Ion chromatography used to identify the charge and number of components present. IC is "…the analysis of ionic analytes by separation on ion exchange stationary phases with eluent

suppression of excess eluent ions," more simply, it is a technique used to separate ions based on their charge (17). Running a sample on the IC involves using hydroxide as an eluent to displace anions from the separator column. By increasing the concentration of the hydroxide during the sample run, various anions are eluted at different retention times, giving rise to different peaks.

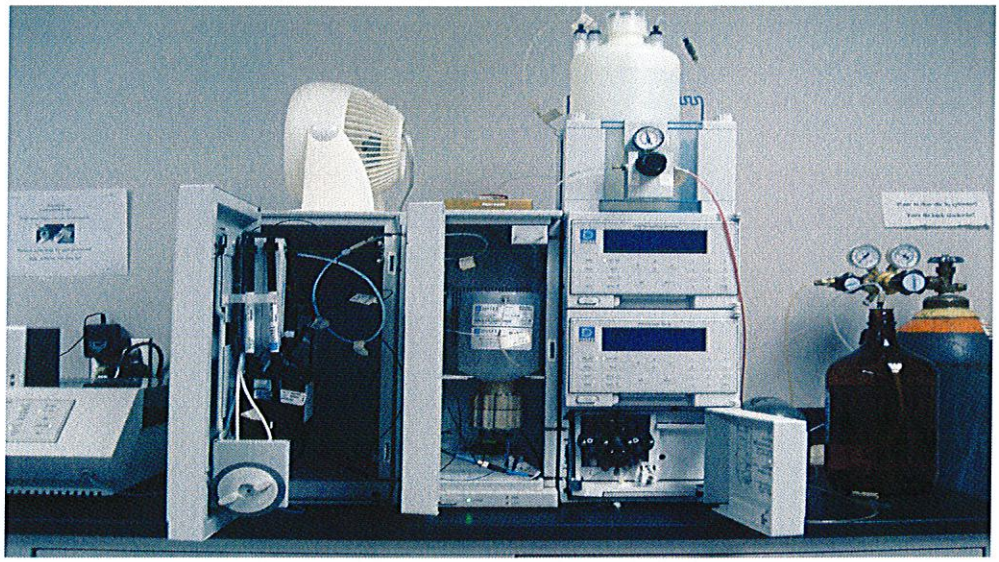

Figure 12. Ion chromatography instrumentation at BSU.

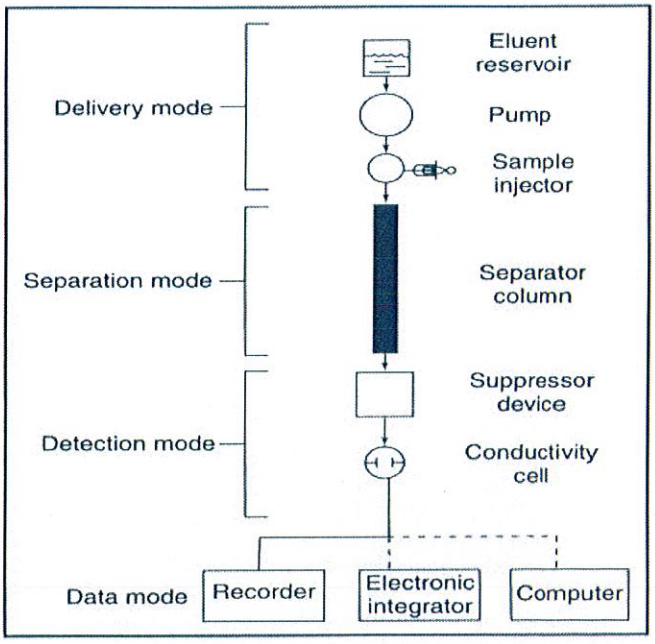

Figure 13. Typical ion chromatography configuration.

"Method detection limits for inorganic anions and cations are typically in the low parts per billion range and recoveries are typically in the low parts per billion range" (9). The linear calibration range extends from low parts per billion to mid parts per million concentrations for most applications" (9). "The main interferences in IC are generally other ions which elute within the timeframe of the ion(s) of interest, and the determination of trace ions in the presence of high levels of other ionic species remains the most difficult of analyses with this technique" (9). With oxoanions, it has been established that lower charges correspond to larger structures. This relationship was thought to allow data to be correlated to the charge determined by ion chromatography with the size of the ion. Information about the charge and size of the ions were initially thought to be used to interpret results from nuclear magnetic resonance (explained in detail later in report) but with further research, data concluded that the IC didn't allow for high enough concentrations to detect for specific components of higher anions. This problem led to further study with the IC and utilizing the various programs the instrument has available to operate. Three specific programs that were used to analyze ions of the three phosphorus containing compounds ($K_4[\alpha\text{-}PV^VW_{11}O_{40}]$, $Cs_6[\alpha\text{-}1,2,3\text{-}PV_3W_9O_{40}]$, and $Cs5[\gamma\text{-}PV_2W_{10}O_{40}]$) included Long, ATP Fast, and Water. Long program consisted of having the longest time period of 42 minutes in which the components of the known and unknown solutions could be analyzed by the instrument. The ATP Fast program provided the fastest analysis of the samples, 16 minutes, by rapidly increasing the amount of hydroxide to be injected into the system. The Water program, a running time of 20 minutes, is the general method used to analyze water samples and was used as another way to critique the analysis. Solutions of a concentration of 400 ppm were used to study the phosphorus containing known and unknown mixtures.

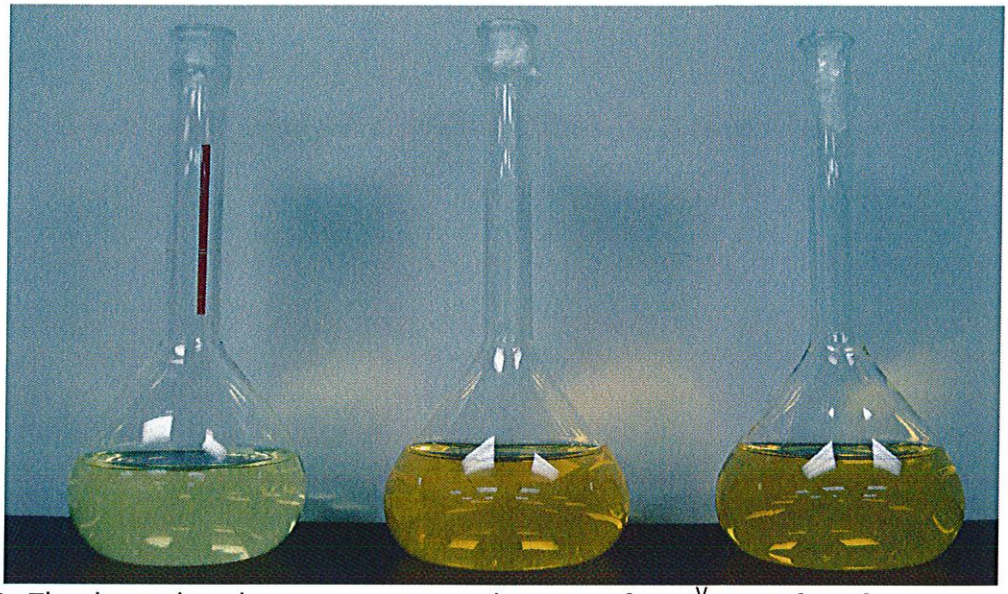

Figure 14. The three phosphorus-containing solutions, $K_4[\alpha\text{-}PV^{V}W_{11}O_{40}]$, $Cs_6[\alpha\text{-}1,2,3\text{-}PV_3W_9O_{40}]$, and $Cs_5[\gamma\text{-}PV_2W_{10}O_{40}]$, made for IC and ^{13}P NMR analysis.

The spectra and data of the samples run with the IC include:

Long Program

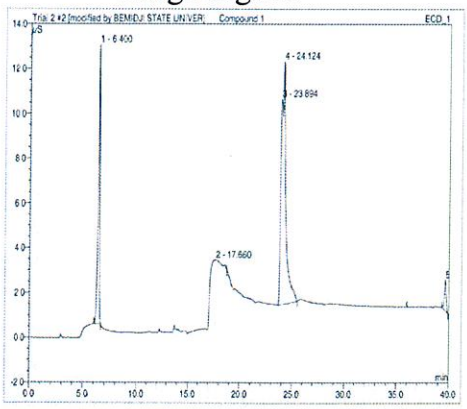

No.	Ret.Time min	Peak Name	Height µS	Area µS*min	Rel.Area %	Amount	Type
1	6.40	n.a.	12.472	1.975	24.96	n.a.	BMB*
2	17.66	n.a.	0.689	0.000	0.00	n.a.	BMB*
3	23.89	n.a.	9.178	2.158	27.28	n.a.	BM
4	24.12	n.a.	10.841	3.517	44.44	n.a.	MB
5	39.64	n.a.	1.345	0.263	3.33	n.a.	BMB*
Total:			34.524	7.913	100.00	0.000	

ATP Fast Program

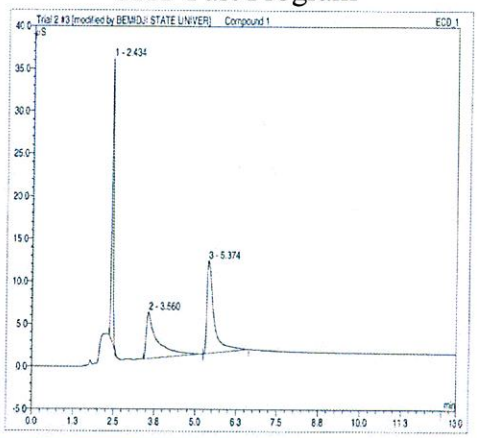

No.	Ret.Time min	Peak Name	Height µS	Area µS*min	Rel.Area %	Amount	Type
1	2.43	n.a.	33.201	1.947	28.45	n.a.	BMB*
2	3.56	n.a.	5.470	2.119	30.98	n.a.	BM*
3	5.37	n.a.	10.836	2.775	40.57	n.a.	MB*
Total:			49.507	6.842	100.00	0.000	

Water Program

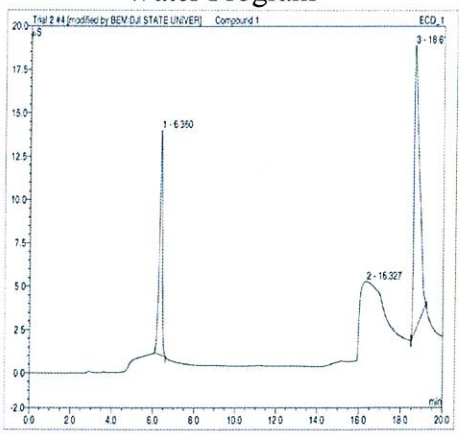

No.	Ret.Time min	Peak Name	Height µS	Area µS*min	Rel.Area %	Amount	Type
1	6.36	n.a.	12.962	2.051	29.44	n.a.	BMB*
2	16.33	n.a.	3.553	0.000	0.00	n.a.	BMB*
3	18.62	n.a.	16.648	4.916	70.56	n.a.	BMB
Total:			33.163	6.967	100.00	0.000	

Figure 15. IC spectra of $K_4[\alpha\text{-}PV^{V}W_{11}O_{40}]$ by the Long, ATP Fast, and Water programs. All three spectra contain the same data except for the retention times, which is due to the different programs used with varying elution times.

Long Program

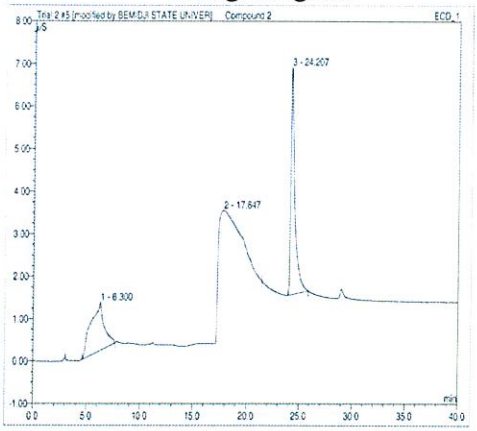

No.	Ret.Time min	Peak Name	Height µS	Area µS*min	Rel.Area %	Amount	Type
1	6.30	n.a.	1.127	1.647	41.69	n.a.	BMB
2	17.85	n.a.	2.037	0.000	0.00	n.a.	BMB*
3	24.21	n.a.	5.338	2.303	58.31	n.a.	BMB
Total:			8.502	3.950	100.00	0.000	

ATP Fast Program

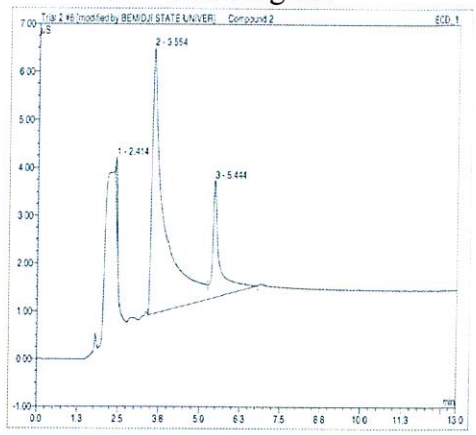

No.	Ret.Time min	Peak Name	Height µS	Area µS*min	Rel.Area %	Amount	Type
1	2.41	n.a.	1.070	0.059	1.89	n.a.	BMB*
2	3.55	n.a.	5.561	2.440	78.19	n.a.	BM
3	5.44	n.a.	2.445	0.622	19.92	n.a.	MB
Total:			9.076	3.121	100.00	0.000	

Water Program

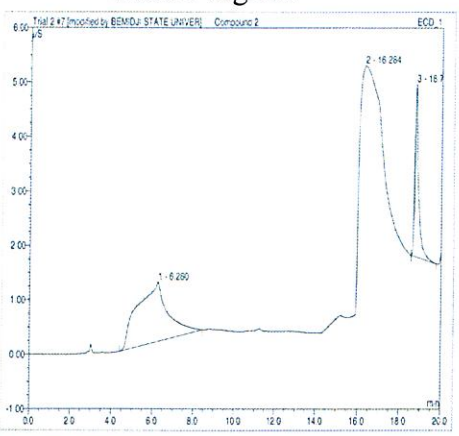

No.	Ret.Time min	Peak Name	Height µS	Area µS*min	Rel.Area %	Amount	Type
1	6.26	n.a.	1.065	1.866	75.83	n.a.	BMB
2	16.28	n.a.	3.803	0.000	0.00	n.a.	BM*
3	18.75	n.a.	3.167	0.595	24.17	n.a.	MB*
Total:			8.054	2.461	100.00	0.000	

Figure 16. IC spectra of $Cs_6[\alpha\text{-}1,2,3\text{-}PV_3W_9O_{40}]$ by the three different programs. All data is the same again, except for the retention times.

Long Program

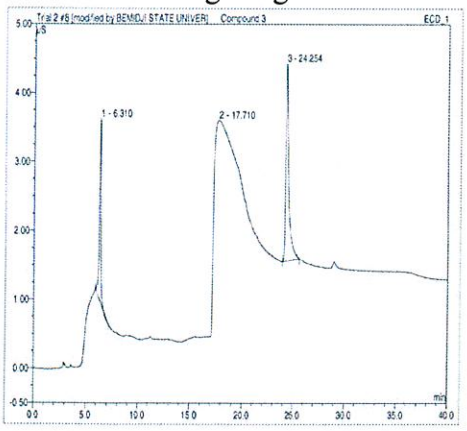

No.	Ret.Time min	Peak Name	Height µS	Area µS*min	Rel.Area %	Amount	Type
1	6.31	n.a.	2.632	0.431	30.61	n.a.	BMB*
2	17.71	n.a.	2.380	0.000	0.00	n.a.	BM*
3	24.25	n.a.	2.863	0.977	69.39	n.a.	MB*
Total:			7.874	1.409	100.00	0.000	

ATP Fast Program

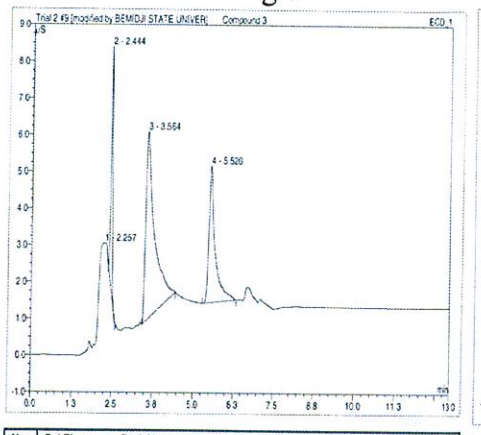

No.	Ret.Time min	Peak Name	Height µS	Area µS*min	Rel.Area %	Amount	Type
1	2.26	n.a.	1.230	0.000	0.00	n.a.	Ru*
2	2.44	n.a.	6.506	0.388	13.91	n.a.	BMB*
3	3.56	n.a.	5.126	1.578	56.50	n.a.	BMB
4	5.52	n.a.	3.713	0.827	29.60	n.a.	BMB
Total:			16.575	2.793	100.00	0.000	

Water Program

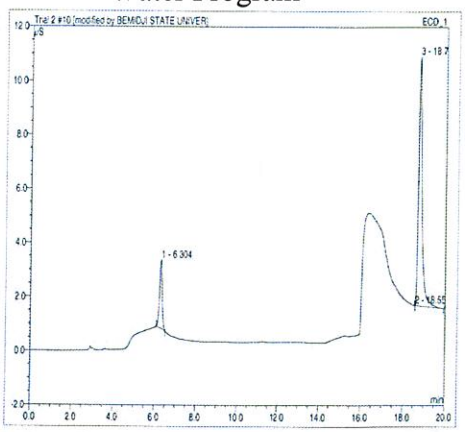

No.	Ret.Time min	Peak Name	Height µS	Area µS*min	Rel.Area %	Amount	Type
1	6.30	n.a.	2.534	0.366	17.62	n.a.	BMB*
2	18.55	n.a.	0.000	0.000	0.00	n.a.	BM*
3	18.73	n.a.	9.237	1.712	82.38	n.a.	MB*
Total:			11.772	2.078	100.00	0.000	

Figure 17. IC spectra of $Cs_5[\gamma\text{-}PV_2W_{10}O_{40}]$ of the three different programs.

Compositions of Unknown Solutions						
Unknown	$K_4[\alpha\text{-}PV^{V}W_{11}O_{40}]$	$Cs_6[\alpha\text{-}1,2,3\text{-}PV_3W_9O_{40}]$	$Cs_5[\gamma\text{-}PV_2W_{10}O_{40}]$	NaCl	Total	Concentration
1	10	10	10	10	40	400 ppm
2	5	15	10	10	40	400 ppm
3	10	15	5	10	40	400 ppm
4	15	5	10	10	40	400 ppm
5	5	10	15	10	40	400 ppm

Table 7. Data given of the compositions of unknown solutions that were analyzed.

Unknown 1
Long Program

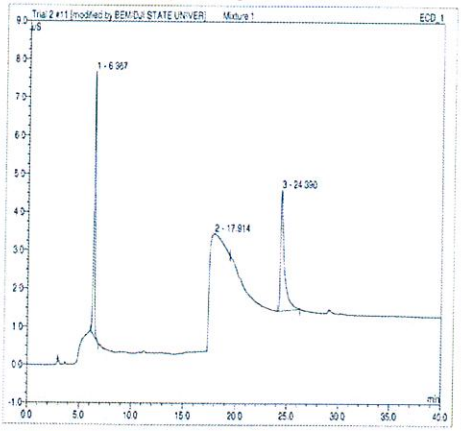

No.	Ret.Time min	Peak Name	Height µS	Area µS*min	Rel.Area %	Amount	Type
1	6.37	n.a.	6.692	1.023	43.45	n.a.	BMB*
2	17.91	n.a.	0.842	0.000	0.00	n.a.	BMB*
3	24.39	n.a.	3.165	1.331	56.55	n.a.	BMB
Total:			10.698	2.354	100.00	0.000	

Unknown 2
Long Program

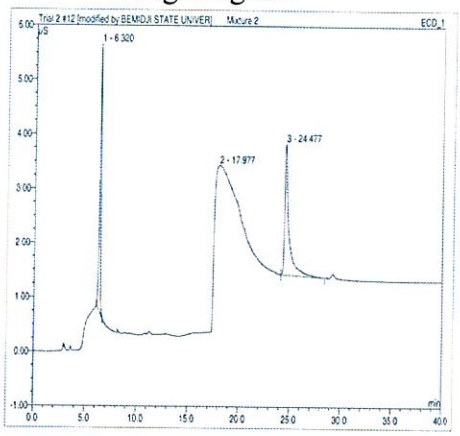

No.	Ret.Time min	Peak Name	Height µS	Area µS*min	Rel.Area %	Amount	Type
1	6.32	n.a.	4.915	0.722	38.65	n.a.	BMB*
2	17.98	n.a.	2.288	0.000	0.00	n.a.	BM*
3	24.48	n.a.	2.411	1.146	61.35	n.a.	MB*
Total:			9.614	1.868	100.00	0.000	

Unknown 3
Long Program

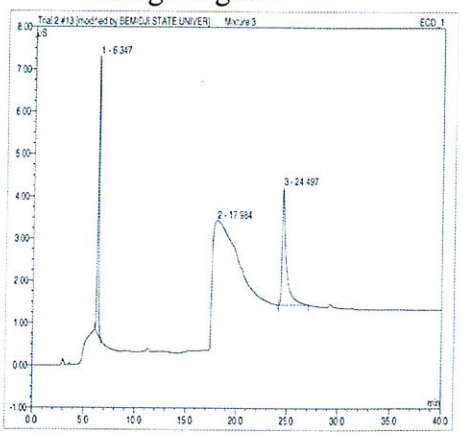

No.	Ret.Time min	Peak Name	Height µS	Area µS*min	Rel.Area %	Amount	Type
1	6.35	n.a.	6.577	0.968	42.59	n.a.	BMB*
2	17.98	n.a.	2.290	0.000	0.00	n.a.	BM*
3	24.50	n.a.	2.795	1.305	57.41	n.a.	MB*
Total:			11.663	2.274	100.00	0.000	

Figure 18. IC spectra of unknowns 1, 2, and 3 run with the three different programs. All three spectra look very similar and have close retention times.

Unknown 4
Long Program

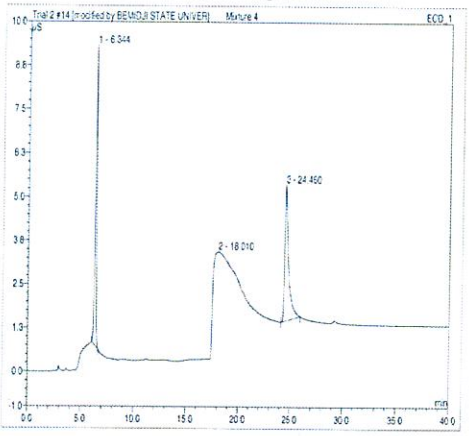

No.	Ret.Time min	Peak Name	Height µS	Area µS*min	Rel.Area %	Amount	Type
1	6.34	n.a.	8.579	1.268	43.03	n.a.	BMB*
2	18.01	n.a.	2.274	0.000	0.00	n.a.	BM *
3	24.46	n.a.	3.895	1.679	56.97	n.a.	MB*
Total:			14.748	2.947	100.00	0.000	

Unknown 5
Long Program

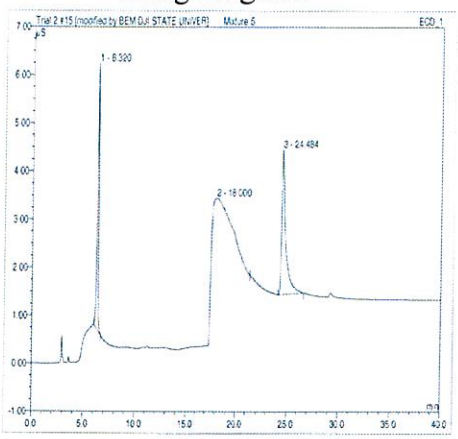

No.	Ret.Time min	Peak Name	Height µS	Area µS*min	Rel.Area %	Amount	Type
1	6.32	n.a.	5.517	0.810	38.11	n.a.	BMB*
2	18.00	n.a.	1.880	0.000	0.00	n.a.	BMB*
3	24.48	n.a.	3.002	1.316	61.89	n.a	BMB
Total:			10.399	2.126	100.00	0.000	

Figure 19. IC spectra of unknowns 4 and 5. Again, they look alike and have the same relative retention times.

After examining the IC data, it appears as though all spectra appear the same with little variations overall. This concludes that the low concentration limits of the IC instrument didn't allow for high enough concentrations to detect for specific components of higher anions. As explained before, the hydroxide that is used to displace the anions off of the stationary phase could have possibly destroyed the structures of the analyzed POMs and created lacunary species. Many things were detected, but all at the same retention time.

Nuclear Magnetic Resonance used as identification of structural information. Nuclear magnetic resonance (NMR) is "the study of absorption of radiofrequency radiation by nuclei in a magnetic field" and is"…an accurate and non-destructive method of determining the structure of molecules in liquids and soluble chemical compounds" (10).

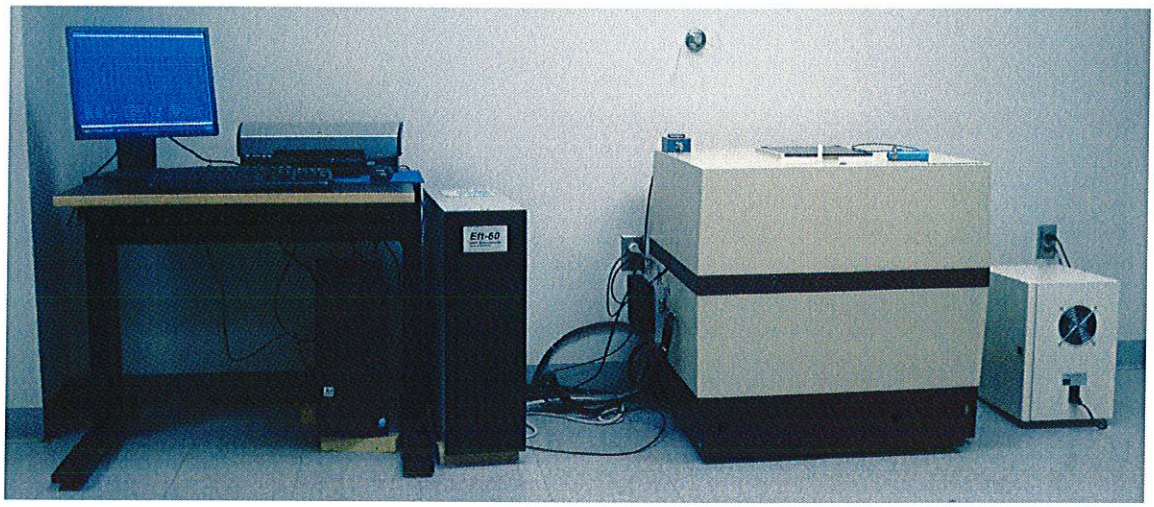

Figure 20. NMR instrumentation at BSU.

NMR detects nuclei that possess a magnetic moment when it is placed in a magnetic field where they are then placed in contact with an oscillating electromagnetic field of the same frequency (3). At this time, energy is produced by the oscillating ratio frequency field that is absorbed by the nuclei spin system (3). Different nuclei have different frequencies and this is why at particular fields, they will absorb energy at certain characteristic radio frequencies (3). For this research of POMs, a certain type of NMR, ^{31}P NMR (phosphorus NMR), was focused on with evaluation of only the phosphorus containing compounds. The 60/90 MHz FT-NMR Instrument, made by Varian (probe manufactured by Anasazi Instruments, Inc.), was used to obtain the ^{13}P NMR data. It was found that little or no work has been done on with ^{13}P NMR and has mostly focused on ^{13}C NMR and ^{1}H NMR (1).

To begin the NMR analysis, phosphoric acid (H_3PO_4) was used to determine a calibration of the lowest possible concentration that could be used to see how far it could be diluted until no data would be observed. The dilutions included, with the observed ^{13}P NMR spectra:

85% Phosphoric Acid Dilutions		
Dilutions:	Molar Concentration, [P]:	Detectable Data:
1 mL → 10 mL	1.470×10^3	Yes
1 mL → 100 mL	1.470×10^2	Yes
1 mL → 1000 mL	1.470×10^1	No

Table 8. Shows the dilutions of 85% phosphoric acid used as a calibration.

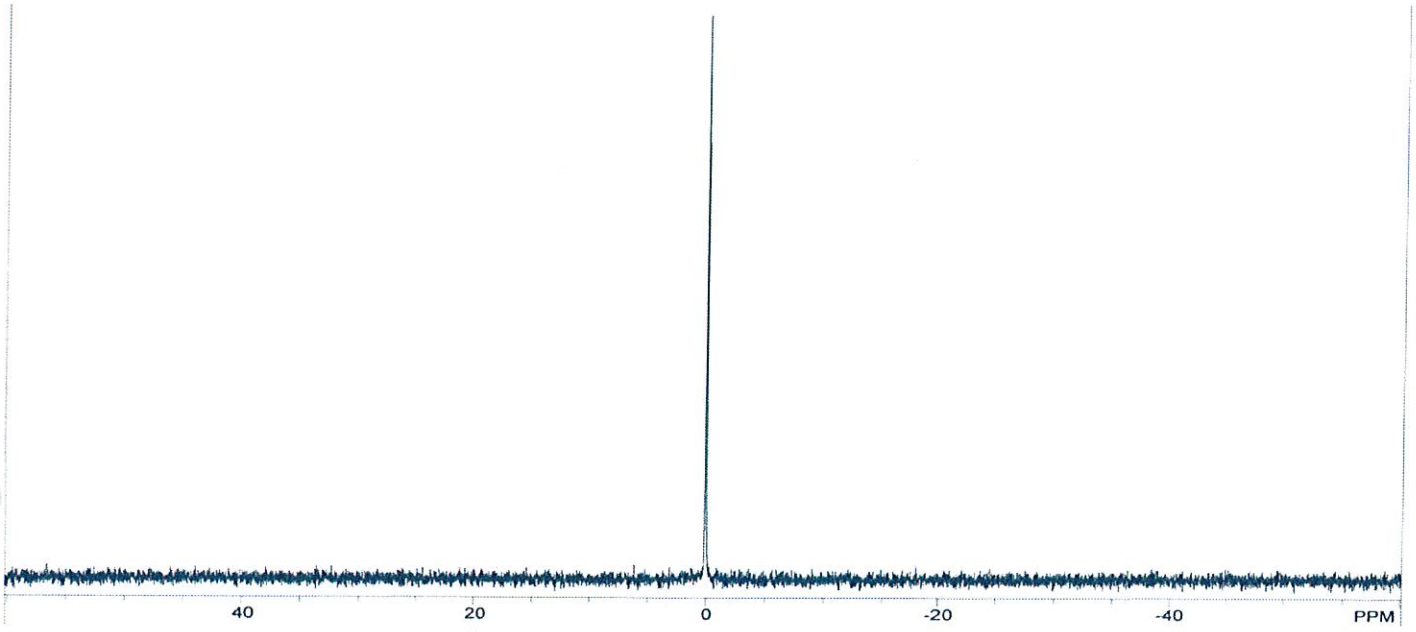

Figure 21. NMR spectrum of 1 mL H_3PO_4 → 10 mL that shows the phosphorus in solution. This peak is very strong indicating the high concentration of phosphorus present. The S/N ratio was 82.0.

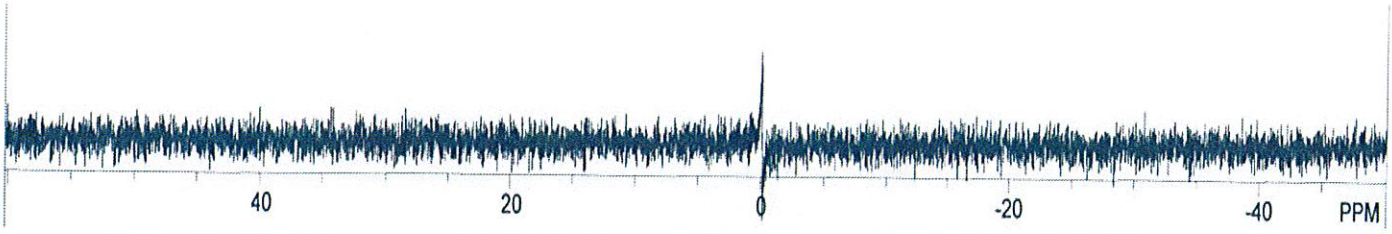

Figure 22. NMR spectrum of 1 mL H_3PO_4 → 100 mL. As compared to figure X, this figure also shows the presence of phosphorus but with a lower concentration due to the relative size of the peak. The S/N ratio was 5.0.

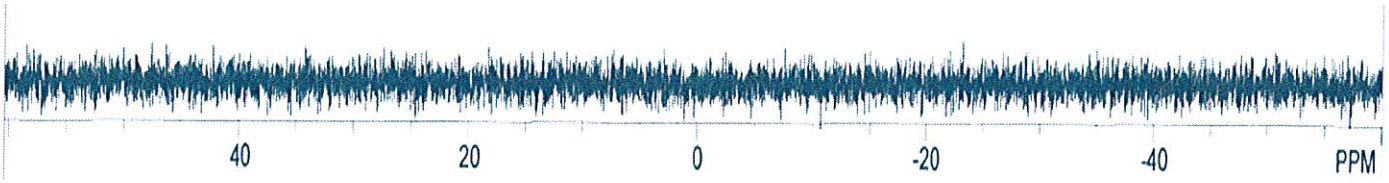

Figure 23. NMR spectrum of 1 mL H_3PO_4 → 1000 mL. This figure shows no presence of phosphorus and just noise. This indicates that at this low of a concentration, the phosphorus is not detectable. The S/N ratio was 1.7.

From here, the solutions previously made of 400 ppm for the IC analysis were used to see if any phosphorus could be detected. With such a low concentration, the ^{13}P NMR spectra resulted with only noise present. This was expected at this point due to the low concentration of 400 ppm. Therefore, new solutions were made with the highest possible solubility in water and yet, no presence of phosphorus was able to be detected.

Next, higher soluble acid forms of POMs (synthesized by Russell Pikal) were used to observe actual phosphorus data by the NMR. The two compounds used were $H_3PMo_{12}O_{40}$ (1 gram soluble in 1 mL of H_2O) and $H_3PW_{12}O_{40}$ (also, 1 gram soluble in 1 mL of H_2O).

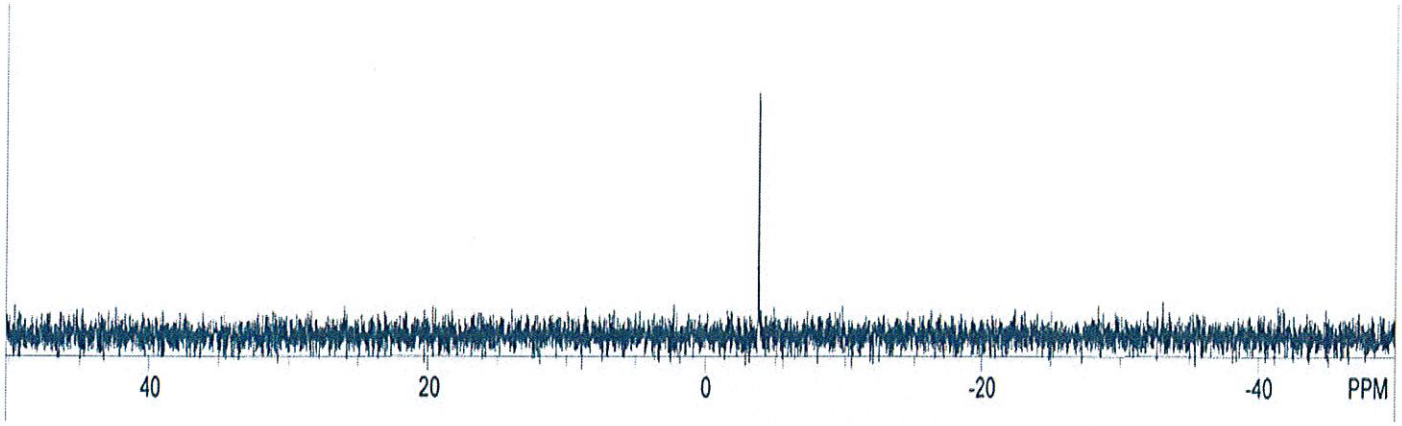

Figure 24. NMR spectra of $H_3PMo_{12}O_{40}$. Peak represents a high concentration of phosphorus present in solution. The S/N ratio was 6.0.

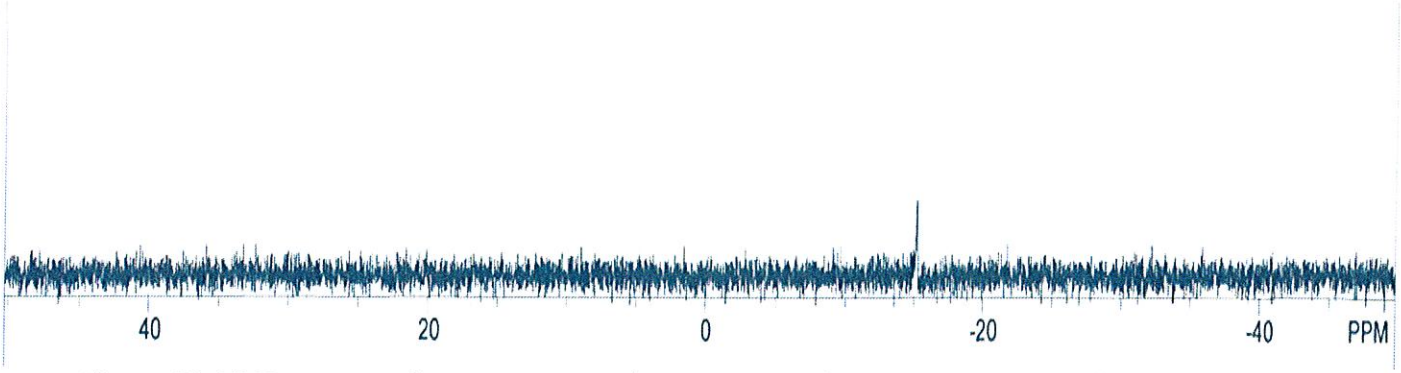

Figure 25. NMR spectra of $H_3PW_{12}O_{40}$. Peak represents a lower concentration than in Figure 24. The S/N ratio ws 3.9.

These two specific POMs were extremely soluble in water because they are salts. With the high water solubility, the concentration of the solution was high enough to detect for the presence of phosphorus. This ^{13}P NMR analysis explains that the concentrations of the desired phosphorus containing POMs were too low for identification.

Conclusions: This research concluded that IR did confirm the identification of desired solids, the IC didn't allow for high enough concentrations to detect for specific components of higher anions, and the ^{13}P NMR showed that the analyzed solutions were soluble in water but at too low of a concentration for detection, thanks in comparison with other researched POMs. Potential, future applications of this specific research includes further work on the unknown solutions for determination of compounds; additional applications of the IC and NMR with the known and unknown solutions; and determining better solubility of the compounds for more inclusive results.

Acknowledgement. Several people would like to be thanked for their time and efforts involved with this research project: Dr. Keith Marek for being my faculty advisor; Garrett Tisdell for his expertise with the use of the IC instrument; Gene Peters for his assistance with obtaining

everything that was necessary for this research; and Russell Pikal for his collaboration in research.

Appendix: Preparation of Analyzed Compounds (6)

Preparation of tetrapotassium α-vanadoundecatungstophosphate, $K_4[\alpha\text{-}PV^VW_{11}O_{40}]$. A 400-mL beaker equipped with a magnetic stir bar and thermometer was charged with 59.004 g of tungstophosphoric acid and 50 mL of deionized water at about 25° C. Small portions of 5.001 g of $LiCO_3$ (lithium carbonate) was added with continuous vigorous stirring to bring the pH of the solution to 4.8 (the pH of the solution was measured by pH paper and a pH meter). The full amount of $LiCO_3$ was needed to adjust the pH to 4.8. In a 250-mL beaker, 3.102 g of $NaVO_3$ (sodium metavanadate) was dissolved in 100-mL of deionized water, with heating at 80° C and a stir bar. Once the solution completely cooled, it was adjusted to a pH of 4.8 by the dropwise addition of ~ 2 mL of 6 M HCl (hydrochloric acid) (the pH being measured by pH paper and a pH meter). This decavanadate solution was then suction filtered through a glass frit and added to the tungstophosphate solution while stirring. The pH of the combined solutions was adjusted to 2.0 with an additional 7 mL of 6 M HCl by dropwise addition. Next, the reaction solution was heated to 60° C for 10 minutes and cooled back down to 25° C, where the pH was then readjusted to 2.0 with 2 mL more of 6 M HCl, and heated up to 60° C again. This process was repeated two more times until the cooled solution remained at a pH of 2.0. One last time, the reaction solution was heated to 60° C, 20.002 g of solid KCl (potassium chloride) was added, and the 60° C temperature was maintained for 15 minutes. The solution was then cooled to 25°C, while stirring, and, at this point, the solution can be described as a canary yellow solid. The colorful solution was suction filtrated through a frit, the solid was washed with two 50-mL portions of

deionized water (having a pH of 2 and at 25°C), and was then dried by suction filtration to produce a yield of 36.946 g.

Preparation of nonasodium nonatungstophosphate, $Na_9[PW_9O_{34}]$. A 150-mL glass beaker was equipped with a stir bar and charged with 60.037 g of $Na_2WO_4{\cdot}2H_2O$ (sodium tungstate dihydrate) and 70.055 g of deionzed H_2O. Once the solid was completely dissolved, 2.0 mL of 85% H_3PO_4 (phosphoric acid) was added dropwise, while stirring, to reach a pH of 9.0. Next, 11.25 mL of CH_3COOH (acetic acid) was added dropwise, with vigorous stirring, and the solution formed a white precipitate, at which the final pH of the solution was 7.2. The solution stirred for an hour and the white precipitate was collected by suction filtration through a glass frit. A yield of 47.265 g was collected.

Preparation of hexacesium α-1,2,3-trivanadononatungstophosphate, $Cs_6[\alpha\text{-}1,2,3\text{-}PV_3W_9O_{40}]$. A 250-mL beaker was obtained, equipped with a magnetic stir bar, and charged with 8.200 g of $NaCH_3COO$ (sodium acetate) and 100 g of deionized H_2O. The solution was stirred until the solid completely dissolved and about 6 mL of CH_3COOH (acetic acid) until a pH of 4.8 was measured with pH paper and a pH meter. To this solution, 3.050 g of $NaVO_3$ (sodium metavanadate) and 20.000 g of $Na_9[PW_9O_{34}]$ (made in previous preparation) was added. The $NaVO_3$ made the solution yellow and the $Na_9[PW_9O_{34}]$ turned the solution to a bright orange. The solution was stirred for 48 hours at 25° C and, over this amount of time, turned to a wine, red-colored solution. The solution was suction filtered with a glass frit to remove any remaining solid. Next, 8.000 g of CsCl (cesium chloride) was dissolved in 10 g of deionized H_2O and added to the filtrate, which turned the filtered solution to an orange color after stirring 30 minutes. The reaction solution was suction filtered and washed with two 50-mL portions of deionized H_2O and dried to yield 17.812 g of orange product.

Preparation of hexacesium pentatungstodiphosphate, $Cs_6[P_2W_5O_{23}]$ and heptacesium decatungstophosphate, $Cs_7[PW_{10}O_{36}]$. In a 600-mL beaker, equipped with a stir bar, 60.000 g of H_2WO_4 (tungstic acid) is combined with 400.000 g of deionized H_2O. About 110 mL of 50% CsOH (cesium hydroxide) was added dropwise with vigorous stirring to the previous solution. The tungstic acid solution was yellow until the addition of the CsOH created a more faint yellow-colored solution. The turbid solution was then passed through 10 g of Celite Analytical Filter aid in a glass frit, which resulted in a colorless solution. The pH of the solution was adjusted to 7.0 with 85% H_3PO_4 (phosphoric acid), that was added dropwise while stirring and the solution stirred for an additional hour. The addition of H_3PO_4 produced a white precipitate. Next, the solution was filtered to give a clear solution and was refrigerated at 0° C for 24 hours until it was filtered again to produce 40.602 g of $Cs_6[P_2W_5O_{23}]\bullet xH_2O$, a white crystalline solid. A 250-mL round-bottom flask was fitted to a reflux condenser and was charged with 150 g of deionized H_2O and 40.602 g of $Cs_6[P_2W_5O_{23}]\bullet xH_2O$. The components were refluxed with heat for 24 hours and then the hot solution was filtered through a glass frit. 15.094 g of this $Cs_7[PW_{10}O_{36}]$ solid resulted. The remaining filtrate was cooled for 48 hours at 0° C and was filtered to yield 1.798 g of unconverted $Cs_6[P_2W_5O_{23}]$.

Preparation of pentacesium γ-divanadodecatungstophosphate, $Cs5[\gamma\text{-}PV_2W_{10}O_{40}]$. A 150-mL beaker was charged with 1.000 g of $NaVO_3$ (sodium metavanadate) and 40.000 g of deionized H_2O to dissolve the solid $NaVO_3$ with the addition of heating to 70° C. Upon cooling to 25° C, 3 M HCl (hydrochloric acid) was added dropwise with strong stirring to lower the pH to 0.8. The reaction solution was a faint yellow. Small portions of the previously made $Cs_7[PW_{10}O_{36}]$ were added, until a total of 12.5 g had been added to the solution. The solution

was then stirred for 30 minutes more and suction filtrated to produce 10.844 g of Cs5[γ-$PV_2W_{10}O_{40}$].

References:

1. "Anasazi Instruments: FT-NMR Instruments for Education and Industry." 15 April 2009 http://www.aiinmr.com.
2. Borrás-Almenar, J.J.; Coronado, E.; Müller, A.; Pope, M. *Polyoxometalate Molecular Science*; Kluwer Academic Publishers: Dordrecht, The Netherlands, 2001.
3. Considine, Glenn D. *Encyclopedia of Chemistry*; John Wiley & Sons: New Jersey, 2005.
4. Cotton, F.A.; Wilkinson, G.; Murillo, C. A.; Bochmann, M. *Advanced Inorganic Chemistry*, 6th ed.; Wiley & Sons: New York, 1999.
5. Day, Victor W. and Walter G. Klemperer. "Metal Oxide Chemistry in Solution: The Early Transition Metal Polyoxoanions." American Association for the Advancement of Science 228 (1985): 533-541.
6. Ginsberg, Alvin P. *Inorganic Syntheses*, Vol. 27; John Wiley & Sons: New York, 1990.
7. Gouzerh, Pierre and Anna Proust. "Main-Group Element, Organic, and Organometallic Derivatives of Polyoxometalates." Chemical Reviews 98, 1 (1998): 77-111.
8. Greenwood, N.N. and A. Earnshaw. *Chemistry of the Elements*; Pergamon Press: New York, 1984.
9. Jackson, Peter E. "Ion Chromatography in Environmental Analysis." *Encyclopedia of Analytical Chemistry*; John Wiley & Sons: Chichester, 2000.
10. Khandpur, R.S. *Handbook of Analytical Instruments*; McGraw-Hill: New York, 2007.
11. Kozhevnikov, Ivan. *Catalysts for Fine Chemical Synthesis: Catalysis by Polyoxometalates*, Vol. 2; John Wiley & Sons: West Sussex, England, 2002.

12. Pope, M.T. *Heteropoly and Isopoly Oxometalates*; Springer-Verlag: Berlin, 1983.

13. Pope, Michael T. "Polyoxometalates." Encyclopedia of Inorganic Chemistry, Second Edition (2008): 4575-4585.

14. Pope, Michael T. and Achim Müller. *Polyoxometalate Chemistry From Topology via Self-Assembly to Applications*; Kluwer Academic Publishers: Norwell, Massachusetts, 2001.

15. Pope, Michael T. and Achim Müller. *Polyoxometalates: From Platonic Solids to Anti-Retroviral Activity*; Kluwer Academic Publishers: Dordrecht, The Netherlands, 1994.

16. Pope, M.; Müller, A.; Borrás-Almenar, J.J.; Coronado, E. *Polyoxometalate Molecular Science*, vol. 98; Kluwer Academic Publishers: Dordrecht, The Netherlands, 2003.

17. Robinson, J.W.; Skelly Frame, E.M.; Frame II, G.M. *Undergraduate Instrumental Analysis*, 6th ed.; Marcel Dekker; New York, 2005.

18. Solomons, T.W. Graham and Craig B. Fryhle. *Organic Chemistry*, 9th ed.; Wiley & Sons: New Jersey, 2008.